Available online at www.sciencedirect.com
ScienceDirect
Journal of Computational Physics 226 (2007) 2063–2077
JOURNAL OF COMPUTATIONAL PHYSICS
www.elsevier.com/locate/jcp

# Convergence stability and estimator in orbital free electronic structure calculation on a grid at finite temperature

S. Le Roux, G. Zérah *

*Département de Physique Théorique et Appliquée, CEA/DAM Ile de France, BP 12, 91680 Bruyères le Chatel, France*

Received 16 October 2006; received in revised form 23 June 2007; accepted 26 June 2007
Available online 6 July 2007

**Abstract**

The electronic charge density is the central quantity in density functional theory. It can be expressed as the diagonal elements of the density matrix in its real space representation, which can be computed by a recursion method based on the Trotter formula. This allows for an orbital free computation of the charge density in the Kohn Sham formalism at finite temperature whose numeric complexity increases linearly with the size of the system (that is, an order N method).

No assessment of the numerical properties such an approach has been presented yet, and this paper aims to analyze its convergence properties.

In particular, we wish to understand its convergence properties as a function of the number of recursion steps, to establish an error estimate in order to devise a stopping criterion, and to analyze the ''locality properties'' of the method which is necessary to make it an order N method. We illustrate the assessment with numerical tests performed for the free electron gas and for Helium at a density and high temperature relevant to shock physics.


*MSC:* 65Z05; 82D10; 81V10

*Keywords:* Electronic structure; Plasmas; Order N method; Recursion

## 1. Introduction

The recursion method has already a long history as a method to compute the density of states in electronic structure calculations [1,2]. It is generally formulated in a tight binding approach, where the small size of the basis set allows for the computation of diagonal and non-diagonal matrix elements of the density matrix in a small computer time. This method has been extended more recently to perform total energy calculations as well as molecular dynamic simulations within the so-called ''bond order potential'' formalism [3]. The method

* Corresponding author.
*E-mail addresses:* stephane.lerouxs@cea.fr (S. Le Roux), gilles.zerah@cea.fr (G. Zérah).

0021-9991/$ - see front matter 
doi:10.1016/j.jcp.2007.06.022

does not require the computation of the wave functions (it is an orbital free method), and is therefore adapted to systems for which such calculations would lead to very large computation times. This is for example the case of high temperature plasmas, where the broadening of the Fermi–Dirac distribution leads to a rapid increase of the number of populated states. This proliferation has so far limited the temperature range which has been covered by *ab initio* molecular dynamics methods where the electrons receive full quantum mechanical treatment and the ions are propagated classically on the resulting energy surface. While this approach has been extensively used in the past ten years in this field and was rather successful at computing the physical properties of dense plasmas, [4–7] it has only been possible to perform simulations above 10 eV or so by resorting to approximate expressions of the kinetic energy functional [8].

Besides tight binding formulations, an alternative setting of the recursion method, more easily extensible toward high temperatures, has been devised by Baroni and Giannozzi [9], in which the electronic density is directly computed on a regular mesh in real space. In their approach, the basis set in made of $\delta$ functions centered on grid points, and the electronic density is computed from the knowledge of the diagonal matrix elements of the resolvent operator of the Hamiltonian for every elements of this basis set. This method is therefore well suited for an implementation in the Kohn–Sham formalism, since the electronic density is the central quantity in this formalism, and the basis set can be easily increased to achieve convergence. Indeed, the basis set might become very large, and this drawback can be somewhat alleviated by the use of massively parallel computers. An extension of this technique to finite temperature has more recently been presented [10] and an application to an hydrogen plasma has been performed by Bagnier, Dallot and one of the authors. In the course of this work we noted that it was not always clear how to terminate the density matrix expansion in continued fraction (the so-called terminator problem, a general difficulty of the recursion method see e.g.[11]). Therefore, a variant of this approach was later elaborated, which relies on a direct evaluation of the diagonal elements of the Fermi density matrix operator at finite temperature. This approach has already been presented in a previous paper [12], but no assessment of its numerical properties were given at the time.

The aim of the present work is to analyze the convergence properties of this latter method in many respects:

- Understand the convergence properties as a function of the number of recursion steps.
- Establish an error estimate to have a criterion for stopping the recursion process.
- Analyze the "locality properties" of the method, this last point being necessary to achieve order N scalability.

The paper is organized as follows: in the next section we recall the salient formulas of the method, and in the next three sections, we give an analysis of the three points mentioned above. In the last section, we illustrate with numerical tests, first for the independent electron gas for which the solution is known, and for Helium on a lattice. For this last system, the thermodynamic conditions are approximately five fold compression, and a temperature of about 13 eV (150,000 K). This corresponds to conditions one might encounter in shock experiments [13], and we compare our density with the one obtained with the Abinit code [14].

## 2. Short description of the method

In this paper, we consider a high temperature plasma, described within the Kohn–Sham–Mermin formalism (see e.g. [15]). In this formalism, the system of $N$ nuclei and $ZN$ electrons is confined in a cubic box, with periodic boundary conditions. Moreover, we will consider the so-called $\Gamma$ point, that is, we will work on the space of periodic wave functions. In other words, all quantities below should be considered as being defined on a torus constructed on the cubic box. In this setting, the electrons are described by a one electron Hamiltonian $H$, given by (in atomic units):

$$H = -\Delta/2 + V(r) \tag{1}$$

where $V(r)$ is the local effective potential. In the sequel, we will describe the nuclei–electron interaction by a smooth local pseudo-potential [16], and we will consider that $V$ is a $\mathbb{C}^\infty$, periodic function defined on our cubic box of size $L$. At finite temperature, the electrons are distributed according to the Fermi–Dirac distribution, given in operator form by:

$$F = \frac{e^{-\beta(H-\mu)}}{1+e^{-\beta(H-\mu)}} \tag{2}$$

where $\beta$ is the inverse temperature and $\mu$ is the chemical potential. At this point, we need some properties of the Fermi–Dirac density matrix to proceed further.

### 2.1. The Fermi–Dirac density matrix

The exponential of the Hamiltonian $e^{-\beta H}$ has been extensively described in the review paper of Simon [17]. In particular, we know that the exponential can be represented by a $\mathbb{C}^\infty$ kernel $K(x,y)$, that is we can write for any function (e.g. in $\mathbb{L}^p$):

$$e^{-\beta H} f(x) = \int K_\beta(x,y) f(y) dy \tag{3}$$

where the density matrix $K_\beta(x,y)$ is a periodic, positive, $\mathbb{C}^\infty$ function in $(x,y)$. The integral, as well as all our functions are defined on a torus. We want to show that the Fermi–Dirac density matrix can be represented in a similar way.

Since $e^{-\beta H}$ is self-adjoint in $\mathbb{L}^2$ with a positive spectrum, the operator $I + e^{-\beta H}$ is invertible, and we have the spectral representation in $\mathbb{L}^2$:

$$\frac{e^{-\beta(H-\mu)}}{1+e^{-\beta(H-\mu)}} = \sum_{i=0}^{\infty} \frac{e^{-\beta(\epsilon_i-\mu)}}{1+e^{-\beta(\epsilon_i-\mu)}} |\phi_i\rangle\langle\phi_i| \tag{4}$$

where $|\phi_i\rangle\langle\phi_i|$ denotes the orthogonal projector on $\phi_i$, the $i^{\text{th}}$ eigenvector of $H$, with eigenvalue $\epsilon_i$.

Now, for each eigenfunction, we can obtain a upper bound by using:

$$|\phi_i(x)| = e^{\beta'\epsilon_i} \left| \int K_{\beta'}(x,y)\phi_i(x)dx \right| \leqslant C_{\beta'} e^{\beta'\epsilon_i} \tag{5}$$

with $C_{\beta'} = \sup_x [\int K_{\beta'}(x,y)^2 dy]^{1/2}$, since $\|\phi_i\|_2 = 1$. A similar upper bound can also be obtained for any derivative of the eigenfunctions. From this upper bound, used with $\beta' < \beta$, we obtain that the series given by:

$$\rho(x,y) = \sum_{i=0}^{\infty} \frac{e^{-\beta(\epsilon_i-\mu)}}{1+e^{-\beta(\epsilon_i-\mu)}} \phi_i(x)\phi_i(y) \tag{6}$$

(and its derivatives) converges uniformly in $(x,y)$,and we therefore have that the Fermi–Dirac density matrix, $\rho(x,y)$, is $\mathbb{C}^\infty$ and satisfies:

$$\frac{e^{-\beta(H-\mu)}}{1+e^{-\beta(H-\mu)}} f(x) = \int \rho(x,y) f(y) dy \tag{7}$$

Finally, the electronic density can be defined in terms of the Fermi–Dirac density matrix as [15]:

$$\rho(x) = \rho(x,x) \tag{8}$$

### 2.2. Outline of the calculation procedure

Our calculations will be performed on a regular cubic orthonormal grid with periodic boundary conditions. Introducing the step size $h$ of the grid, the basis vectors $v_0^{i,h}$, are piecewise constant functions defined as

$$v_0^{i,h}(\mathbf{r}_j) = \frac{\delta_{ij}}{h^3} = \begin{cases} h^{-3} & \text{if } i = j \\ 0 & \text{if } i \neq j \end{cases}$$

And the electronic density is approximated as

$$\rho_h(\mathbf{r}_i) = \left\langle v_0^{i,h} \middle| \frac{e^{-\beta(H-\mu)}}{1+e^{-\beta(H-\mu)}} \middle| v_0^{i,h} \right\rangle = \left( \langle v_0^{i,h}|1|v_0^{i,h}\rangle - \left\langle v_0^{i,h} \middle| \frac{1}{1+e^{-\beta(H-\mu)}} \middle| v_0^{i,h} \right\rangle \right)$$

In view of the fact that the Fermi–Dirac operator possesses a $\mathbb{C}^\infty$ kernel, this approximation converges at least as $h^2$ if we take $\mathbf{r}_i$ as the mid point of our discretization grid, in which case,

$$\left|\frac{1}{h^6}\int_{\Omega_h}\int_{\Omega_h}\rho(x,y)\mathrm{d}x\,\mathrm{d}y-\rho(\mathbf{r}_i)\right|\leqslant Ch^2 \tag{9}$$

and the integral is computed over $\Omega_h$ the support of $v_0^{i,h}$. We note at this point that different basis functions, as e.g. gaussians could be used and yield more accurate results at the expense of a more complicated implementation. To evaluate the last term of this expression, we transform it in tridiagonal form, on a basis whose first vector is $u_0^{i,h}=h^{3/2}v_0^{i,h}$ according to the Lanczos procedure ($u_{-1}^{i,h}=u_0^{i,h}$):

$$\mathrm{e}^{-\beta(H-\mu)}u_n^{i,h}=b_n^{i,h}u_{n-1}^{i,h}+a_n^{i,h}u_n^{i,h}+b_{n+1}^{i,h}u_{n+1}^{i,h}$$

In this expression, the $u_n$ are orthonormal (hence the $h^{3/2}$ factor in front of $h^{3/2}v_0^{i,h}$) and the coefficients of the recursion satisfy:

$$a_n=\langle u_n|\mathrm{e}^{-\beta(H-\mu)}|u_n\rangle$$
$$b_n=\langle u_{n-1}|\mathrm{e}^{-\beta(H-\mu)}|u_n\rangle$$

(In the sequel and for clarity we will drop unless specified the indexes $i$ and $h$ in $a_n^{i,h}$ and $b_n^{i,h}$ and $u_n^{i,h}$.) The density at $\mathbf{r}_i$ is the diagonal matrix element of the Fermi density matrix and can therefore be expanded in a continued fraction as [18]:

$$h^3\rho_h(\mathbf{r}_i)=1+\cfrac{1}{-1-a_0-\cfrac{b_1^2}{-1-a_1-\cfrac{b_2^2}{\ddots}}} \tag{10}$$

noted $1+\sum_{k=0}^{\infty}(-b_k^2)|(-1-a_k)$.

As we will show below, the use of the exponential of $H$ (instead of $H$ directly as in the original method) presents some advantages in particular concerning the termination of the continued fraction (see (4)), but also some drawbacks. In particular, the evaluation of an exponential can be quite expensive, a difficulty which is bypassed in [12], by using the Trotter formula in a partial fraction decomposition of the Fermi density matrix. Specifically, we recast the Fermi density matrix as a sum of Fermi density matrices at a higher temperature $2pT$, where $p$ is an integer, and shifted chemical potential using the formula:

$$\frac{1}{1+\mathrm{e}^{-\beta(H-\mu)}}=\frac{1}{2p}\sum_{j=0}^{2p-1}\frac{1}{1+z_j\mathrm{e}^{-\frac{\beta(H-\mu)}{2p}}}=\frac{1}{2p}\sum_{j=0}^{2p-1}\frac{z_j}{z_j-\mathrm{e}^{-\frac{\beta(H-\mu)}{2p}}} \tag{11}$$

where, $z_j=\exp(\mathrm{i}\pi(2j+1)/2p)$.

For large $p$, we can use the Trotter formula (or, more accurately, the symmetric Feynmann–Strang splitting) and approach the operator $\mathrm{e}^{-\frac{\beta(H-\mu)}{2p}}$ by the product of three operators, that is:

$$\mathrm{e}^{-\frac{\beta(H-\mu)}{2p}}\simeq\mathrm{e}^{\frac{\beta\mu}{2p}}\mathrm{e}^{-\frac{\beta V}{4p}}\mathrm{e}^{\frac{\beta\Delta}{4p}}\mathrm{e}^{-\frac{\beta V}{4p}} \tag{12}$$

The action on a vector $|u>$ of each term of this product can then be rapidly evaluated.

The consequences of these transformations on the precision and on the convergence properties on the method have not yet been analyzed, and our aim is to present in this paper some results in this direction.

We will particularly concentrate on the simulation of plasmas at finite temperature, a system for which the method is particularly well suited.

## 3. The effect of the Feynmann–Strang splitting

When using the expansion (11), in order to evaluate $\left\langle v^h\left|\frac{1}{1+\mathrm{e}^{-\beta(H-\mu)}}\right|v^h\right\rangle$ we need to evaluate terms of the form: $\left\langle v^h\left|\frac{1}{1+z_j\mathrm{e}^{-\frac{\beta(H-\mu)}{2p}}}\right|v^h\right\rangle$. To this end, we replace the exponential $T=\mathrm{e}^{-\frac{\beta(H-\mu)}{2p}}$, in the denominator of this last term by the splitting $S=\mathrm{e}^{\frac{\beta\mu}{2p}}\mathrm{e}^{-\frac{\beta V}{4p}}\mathrm{e}^{\frac{\beta\Delta}{4p}}\mathrm{e}^{-\frac{\beta V}{4p}}$.

Using formula (11) again, but now with $S$ instead of $T$, the error induced by using the splitting is given by $\langle v^h|\delta|v^h\rangle$, with:

$$\delta = \frac{1}{1+T^n} - \frac{1}{1+S^n} \tag{13}$$

where we change in this section, the notation $2p$ by $n$. Since $v^h$, is bounded in $\mathbb{L}^1$ uniformly in $h$, to achieve an upper bound of $|\langle u_h|\delta|u_h\rangle|$ independent of $h$, we need to bound objects of the form $|\langle f|\delta|g\rangle|$ in terms of the $\mathbb{L}^1$ norm of $f$ and $g$.

The convergence of the difference $S - T$ as a function of the inverse temperature has been recently studied, and results have been obtained in the literature in the $\|\ \|_{p,p}$ norms, that is their norms as operators from $\mathbb{L}^p$ to $\mathbb{L}^p$.

We will use the following result, whose proof, in different settings can be found in [19–21]:

**Proposition 1.** *If the effective potential is a $\mathbb{C}^\infty$ function defined on a torus, we have $\|S - T\|_{p,p} \leqslant C(\beta/n)^2$, for $1 \leqslant p < \infty$.*

Since both $f$ and $g$ are bounded in $\mathbb{L}^1$, those results are not sufficient, and we need upper bounds in the $\|\ \|_{p,q}$ norms.

Let us now study our operator $\delta$, when using the $\mathbb{L}^\infty$ norm.

We first note that since the spectrum of $T^n$ and $S^n$ are positive, the operators $I + T^n$ and $I + S^n$ are invertible in $\mathbb{L}^2$, and the norm of their inverse is bounded by 1, that is $\|(I + T^n)^{-1}\|_2 \leqslant 1$ and $\|(I + S^n)^{-1}\|_2 \leqslant 1$.

We now rewrite our difference (using Dyson's formula):

$$\delta = \frac{1}{1+T^n} - \frac{1}{1+S^n} = -\frac{1}{1+T^n}(T^n - S^n)\frac{1}{1+S^n} \tag{14}$$

and in a similar fashion as in [20]

$$\delta = -\frac{1}{1+T^n}\sum_{j=0}^{n-1} T^{n-j-1}(T-S)S^j\frac{1}{1+S^n} \tag{15}$$

$$= -\sum_{j=0}^{n-1} T^{n-j-1}\frac{1}{1+T^n}(T-S)\frac{1}{1+S^n}S^j \tag{16}$$

To obtain our result, that is norms of the $\|\ \|_{p,q}$ type, we will use the basic theorem (see e.g. [17]):

**Theorem 1.** *If $\beta$ belongs to a compact set of $\mathbb{R}$ , we can find a constant $C$, independent of $\beta$ such that*

$$||\mathrm{e}^{-\beta H}||_{p,q} < \frac{C}{\beta^\gamma} \text{ with } \gamma = \frac{3}{2}\left\{\frac{1}{p} - \frac{1}{q}\right\} \text{ and } 1 \leqslant p \leqslant q \leqslant \infty \tag{17}$$

**Proof.** See [17]. □

We will use two particular cases:

$$||\mathrm{e}^{-\beta H}||_{1,\infty} < \frac{C}{\beta^{3/2}}$$

and

$$||\mathrm{e}^{-\beta H}||_{1,2} < \frac{C}{\beta^{3/4}}$$

When $V(x)$ is $\mathbb{C}^\infty$ on a torus, similar bounds can be obtained for the Feynmann–Strang splitting $S$, since $(Sf)(x) = \mathrm{e}^{-\beta V(x)/2}\int K^0_\beta(x,y)\mathrm{e}^{-\beta V(y)/2}f(y)\mathrm{d}y$, where $K^0_\beta(x,y)$ is the (positive) kernel associated with $\mathrm{e}^{\beta\Delta/2}$, and the terms $\mathrm{e}^{-\beta V(y)/2}$ is bounded in $\mathbb{L}^\infty$. The same line of reasoning can be applied to $S^j$ where $j$ is an integer.

We can now state our result:

**Proposition 2.** *If the potential is $\mathbb{C}^\infty$ is defined on a three dimensional torus we can find a constant $C$, such that, for any $f$ and $g$ in $\mathbb{L}^1$ we have, for $n > 1$:*

$$|\langle f|\delta|g\rangle| < C\frac{\beta^{1/2}}{n}||f||_1||g||_1$$

**Proof.** Of the terms appearing in the sum (16) we first consider terms for which $j \neq 0$ and $j \neq n-1$. □

We have

$$||S^j||_{1,2} < \frac{C}{(j\beta/n)^{3/4}} \quad \text{and} \quad ||T^{n-j-1}||_{1,2} < \frac{C}{[((n-j-1)\beta/n)^{3/4}]}$$

and since the $\|\ \|_{2,2}$ norm of $T-S$ is bounded by $(\frac{\beta}{n})^2$ and we have the upper bounds $\|(I+T^n)^{-1}\|_2 < 1$, and $\|(I+S^n)^{-1}\|_2 < 1$:

$$\langle f|T^{n-j-1}(I+T^n)^{-1}(T-S)(I+S^n)^{-1}S^j|g\rangle \tag{18}$$

$$\leqslant C\frac{\beta^{1/2}}{n^2}\frac{1}{(j/n)^{3/4}[((n-j-1)/n)^{3/4}]}||f||_1||g||_1 \tag{19}$$

The sum over of those terms yields:

$$\frac{\beta^{1/2}}{n^2}\sum_{j=1}^{j=n-2}\frac{1}{(j/n)^{3/4}[((n-j-1)/n)^{3/4}]} \leqslant C\frac{\beta^{1/2}}{n} \tag{20}$$

Since,

$$\frac{1}{n}\lim_{n\to\infty}\sum_{j=1}^{j=n-2}\frac{1}{(j/n)^{3/4}[((n-j-1)/n)^{3/4}]} = \int_0^1 \frac{\mathrm{d}x}{x^{3/4}(1-x)^{3/4}} < \infty \tag{21}$$

We now consider the terms with $j=0$ or $j=n-1$, and give the details for the $j=0$ term only. This term can be written:

$$\left\langle f\left|\frac{T^{n-1}}{1+T^n}(T-S)\frac{1}{1+S^n}\right|g\right\rangle = \left\langle f\left|T^{n-1}\frac{1}{1+T^n}(T-S)\frac{S^n}{1+S^n}\right|g\right\rangle - \left\langle f\left|T^{n-1}\frac{1}{1+T^n}(T-S)\right|g\right\rangle$$

The first term of the right hand side can be treated as above, and yields a upper bound in $\frac{\beta^{1/2}}{n^2}$, and for the second term, using a similar transformation, we need to consider:

$$\left\langle f\left|\frac{T^{n-1}}{1+T^n}(T-S)\right|g\right\rangle = \langle f|T^{n-1}(T-S)|g\rangle - \left\langle f\left|\frac{T^{2n-1}}{1+T^n}(T-S)\right|g\right\rangle$$

For the first term, we use the $\mathbb{L}^1$ norm of $(T-S)$: $\|T-S\|_1 < C(\beta/n)^2$ and (for $n>1$) the norm of $T^{n-1}$: $\|T^{n-1}\|_{1,\infty} \leqslant C\frac{1}{\beta^{3/2}}$ to obtain:

$$< f|T^{n-1}(T-S)|g > \leqslant C\frac{\beta^{1/2}}{n^2}||f||_1||g||_1 \tag{22}$$

We finally write the second term as

$$-\left\langle f\left|T^{n-1}\frac{1}{1+T^n}T^n(T-S)\right|g\right\rangle \tag{23}$$

and obtain, using $\|\ \|_{1,2}$ norms of $T^{n-1}, T^n$, the $\mathbb{L}^2$ norm of $\frac{1}{1+T^n}$ and the $\mathbb{L}^1$ norm of $(T-S)$ again a upper bound by $C\frac{\beta^{1/2}}{n^2}||f||_1||g||_1$.

We note that two points are not treated in the present Proposition. First, the case $n=1$ requires a different approach, using techniques developed in the already cited references. Second, it might be possible to obtain a better scaling, as e.g. $\frac{\beta^{1/2}}{n^2}$, using lines of the types presented in the paper by [20]. We leave this for a future work.

## 4. Terminator of the continued fraction

The continued fraction (Eq. (10)) is in principle infinite, but in practice must be terminated, and it is customary to replace the sum of the remaining terms of the fraction by a terminator $T(z)$ deduced from some closure relation. In standard applications of the recursion method, when the Hamiltonian itself is tridiagonalized, devising a terminator is a difficult procedure. This is in contrast to our case, where we can show that the recursion coefficients applied to the exponential tend to zero and setting $T(z) = 0$ yields excellent convergence properties.

As already stated, $e^{-\beta(H-\mu)}$ possesses a discrete spectrum given by $\lambda_i = e^{-\beta(\epsilon_i-\mu)}$ which tend to zero at infinity. Therefore, $e^{-\beta(H-\mu)}$ is compact and this is a sufficient condition to insure that the recursion coefficients $a_n$, $b_n$ tend to zero.

Moreover, the operator is trace class [17] and from this we have a very simple proof of this result. Indeed:

$$Tr(e^{-\beta H}) = \sum_n a_n < \infty$$
$$Tr(e^{-2\beta H}) = \sum_n a_n^2 + 2\sum b_n^2 < \infty$$

Although the recursion method is, generally speaking, rapidly convergent [22], this has been shown to be the case for integrated quantities such as the density of states. We here consider directly the electronic density, which is slowly convergent a quantity. Indeed, when trying to devise error estimates in the next section we will directly see that the convergence of $b_n$ toward zero is an essential property.

## 5. An asymptotic estimate of the continued fraction

The next step in the study of the convergence properties of the method is to develop an error estimate of the density as a function of the rank of recursion. It has not been possible to find such a bound, but we have found an asymptotic estimate of the error as a function of the recursion coefficients which is empirically very good. This estimate will be shown to be expressed as a simple function of the current values of $a_n$ and $b_n$, and this therefore allows to stop the calculation when a prescribed precision has been achieved.

To present the error estimate, we start by a general result about continued fractions. Consider:

$$\frac{1}{A_0 + \frac{B_1}{A_1 + \frac{B_2}{A_2 + \cdots + \frac{B_n}{A_n}}}} =: \frac{N_n}{D_n}$$

where $N_n$ and $D_n$ verify the recurrence formulas:

$$N_0 = 1 \qquad D_0 = A_0$$
$$N_1 = A_1 \qquad D_1 = A_0A_1 + B_1$$
$$N_n = A_nN_{n-1} + B_nN_{n-2} \qquad D_n = A_nD_{n-1} + B_nD_{n-2}$$

Now, it is more transparent to write the fraction as a series:

$$\frac{N_n}{D_n} - \frac{N_0}{D_0} = \sum_{k=1}^{n} S_k \quad \text{where } S_k = (-1)^k \frac{\prod_{i=1}^{k} B_i}{D_kD_{k-1}} \tag{24}$$

In the case where the recursion coefficients are positive, the series $S_k$ is alternating and decreasing in absolute value as can easily seen by considering $|\frac{S_n}{S_{n+1}}|$, together with the recurrence relation for $D_n$.

$$\left|\frac{S_n}{S_{n+1}}\right| = \frac{D_{n+1}}{D_{n-1}B_{n+1}} = \frac{A_{n+1}D_n + B_{n+1}D_{n-1}}{D_{n-1}B_{n+1}} \geqslant 1 \tag{25}$$

It is then convergent toward a limit $l$ we then have the classical upper bound:

$$\left|\frac{N_n}{D_n} - l\right| \leqslant |S_{n+1}| = \frac{\prod_{i=1}^{n+1} B_i}{D_n D_{n+1}}$$

It turns out, that in our case where the coefficients are not positive, this upper bound can be turned in an asymptotic estimate (for which use is made of the convergence of the $b_n$):

$$\left|\frac{N_n}{D_n} - l\right| = \frac{\prod_{i=1}^{n+1} b_i^2}{|D_n D_{n+1}|}\left(1 + O(b_{n+2}^2)\right) \tag{26}$$

A proof of this asymptotic expansion, which is somewhat technical is given in the Appendix.

## 6. Locality property

Finally, an important aspect of order N methods, is the locality property. In the case of a local potential, the recursion vector $u_n$, is confined to a region of space whose radius increases like a diffusion process with the number of recursion steps.

For example, in the case of the electron gas, since we use the exponential of the Hamiltonian to construct the recursion basis, the recursion vector belongs to the space spanned by $(u_0, e^{\frac{\beta}{2p}(\frac{\Delta}{2}+\mu)}u_0, \ldots, e^{n\frac{\beta}{2p}(\frac{\Delta}{2}+\mu)}u_0)$. Since $u_0$ is an approximation of a Dirac distribution, the $e^{k\frac{\beta}{2p}\left(\frac{\Delta}{2}+\mu\right)}u_0$ are Gaussian and the support (up to a certain tolerance) of the recursion vector is the same as the support of the widest Gaussian, that is $e^{n\frac{\beta}{2p}\left(\frac{\Delta}{2}-\mu\right)}u_0$. Therefore, if we *a priori* estimate the number of recursion steps is needed, we will be able to limit *a priori* the support of the recursion vectors and therefore effectively localize our calculations around a certain finite neighborhood of each point in space. Unfortunately, the estimate (Eq. (26)) requires the knowledge of the recursion coefficients, and is therefore not an *a priori* estimate. On the other hand, for the case of Helium, we empirically noticed that the number of recursion steps weakly depends upon the point where the density is computed, allowing to effectively localize the recursion vector. In practice, we therefore apply the Hamiltonian in a region of space wide enough to accommodate the maximum expected support of the recursion vectors convoluted by the Gaussian $e^{\frac{\beta}{2p}\left(\frac{\Delta}{2}+\mu\right)}u_0$.

## 7. Numerical studies of the convergence properties

In this section, we will study numerically the convergence of the method with respect to the different parameters in the case of the electron gas and Helium in the condition of strong laser shock experiments [13]. We will first study the convergence with respect to the number of recursion steps, and then compare it with our error estimate. Finally, we will analyze the effect of a localization of $u_n$.

### 7.1. The free electron gas

The free electron gas in a periodic cubic box of length $L$, in the space of periodic wave functions ($\Gamma$ point) allows us to investigate the convergence properties of the method. For a given chemical potential and temperature, the eigenenergies, corresponding wave functions and electronic density are given by [23]:

$$\epsilon_{n_1,n_2,n_3} = \frac{2\pi^2}{L^2}\left(n_1^2 + n_2^2 + n_3^2\right)$$

$$\psi_{n_1,n_2,n_3}(r) = \frac{1}{L^{3/2}}\exp\left(\mathrm{i}\frac{2\pi}{L}(n_1 x + n_2 y + n_3 z)\right)$$

$$\rho = \frac{1}{L^3}\sum_{n_1,n_2,n_3}\frac{1}{1+\exp\left(\beta\left(\frac{2\pi^2}{L^2}(n_1^2+n_2^2+n_3^2) - \mu\right)\right)}$$

The operator $e^{-\beta\left(-\frac{\Delta}{2}-\mu\right)}$ is expressed in real space as a convolution with a normalized Gaussian:

$$e^{-\beta\left(-\frac{\Delta}{2}-\mu\right)}\delta_0 = e^{\beta\mu}T_\beta \quad \text{with } T_\beta(\mathbf{r}) = \left(\frac{1}{2\pi\beta}\right)^{\frac{3}{2}} e^{-\frac{1}{2\beta}|\mathbf{r}|^2}$$

The discretization step $h$ must be chosen in order to yield a good representation of $T_\beta$, and therefore must be proportional to $\sqrt{\beta}$ to yield a constant precision. In Fig. 1 we display the convergence of the density as a function of the recursion order for different discretization steps $h$, for a system at a temperature $T = 150{,}000$ K, in a box of size $L = 30$ Bohr and a chemical potential taken as $\mu = 0$. The first information that can be drawn from the figure is that the method is accurate: for sufficiently small a discretization step (here smaller than 0.75 Bohr) the method converges toward the exact result up to machine precision and it takes less than 5 steps to have an error on the density less than $10^{-8}$.

If we now consider a larger step size (up to 1.2, in Fig. 1), the convergence rate toward the exact density remains the same up to a point beyond which the error remains constant as a function of the recursion order: that is an indication of the stability of the method.

Although we do not need to use the Trotter formula for the free electron gas, it is interesting to see how the method behave when we use this formula with finite values of $p$. In this case we expect that the convergence of the various terms of the sum (11) are different, since for large $p$ some $z_i$ approach 1 and $1 - e^{-\frac{\beta(\epsilon_i-\mu)}{2p}}$ becomes very small when $\frac{\beta(\epsilon_i-\mu)}{2p}$ is small. Moreover, the Gaussian is now given by

$$e^{-\frac{\beta}{2p}\left(-\frac{\Delta}{2}-\mu\right)}\delta_0 = e^{\frac{\beta}{2p}\mu}T_{\frac{\beta}{2p}} \quad \text{with } T_{\frac{\beta}{2p}}(\mathbf{r}) = \left(\frac{p}{\pi\beta}\right)^{\frac{3}{2}} e^{-\frac{p}{\beta}|\mathbf{r}|^2}$$

and are therefore of a smaller variance. Then with a given discretization step, the final discretization error should increase with $p$, and those two effects combine to deteriorate the convergence properties. That result is shown on Fig. 2: with an increasing Trotter parameter, the rate of convergence is decreased and, when the parameter is too large, the maximum achievable precision is diminished. For instance, a Trotter parameter of 25 yields in this case a $10^{-7}$ relative precision after 25 steps, which could be improved further by reducing the step size and increasing the number of recursion steps.

In fact, we found empirically that the speed of convergence is inversely proportional to $\sqrt{p}$.

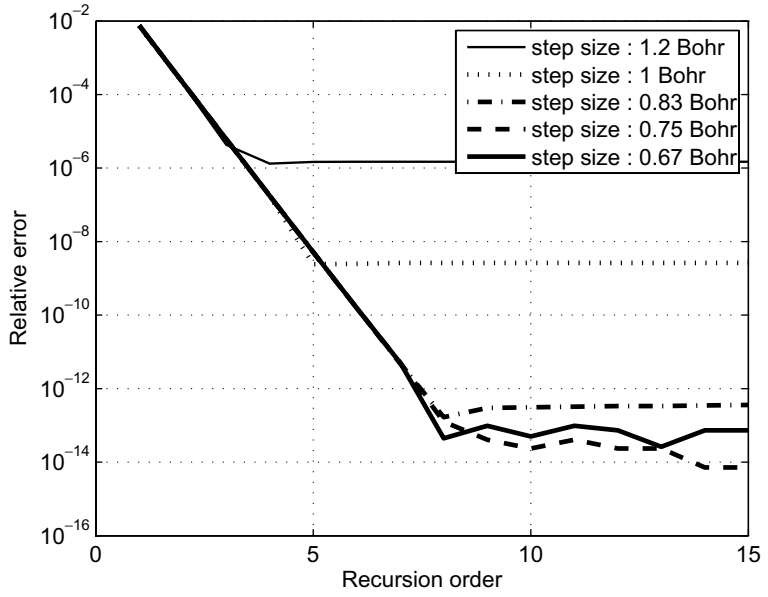


Fig. 1. Convergence of recursion method for the free electron gas toward its exact value for different values of the discretization step $h$. The calculation refers to an electron gas at 150,000 K, a cubic box of size 30 Bohr and a chemical potential taken as $\mu = 0$.

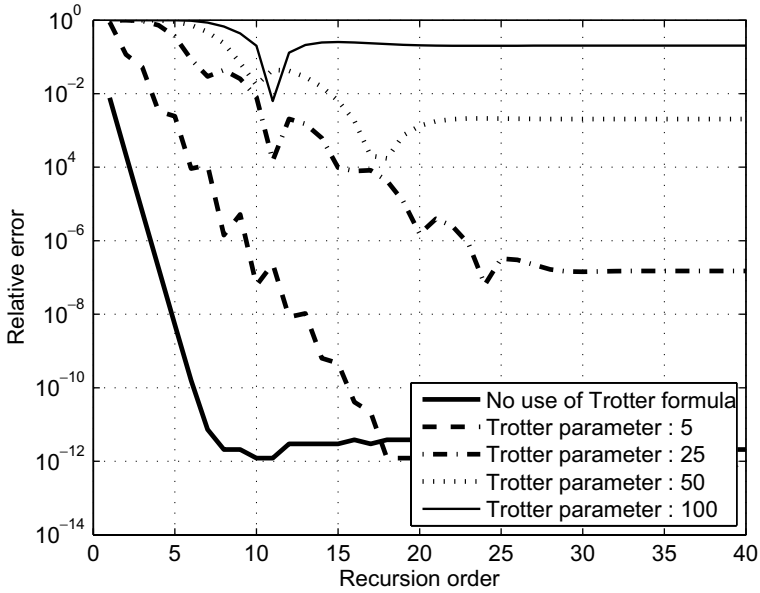


Fig. 2. Convergence of recursion method for the free electron gas for different values of the Trotter parameter. The calculation refers to an electron gas at 150,000 K, a cubic box of size 30 Bohr and a chemical potential taken as $\mu = 0$; the discretization step is 0.2 Bohr.

### 7.2. Helium CFC

We will now present some tests for a realistic system, that is using a non-zero potential. We compare the density computed by the present method and the density computed by Abinit, a code for performing electronic

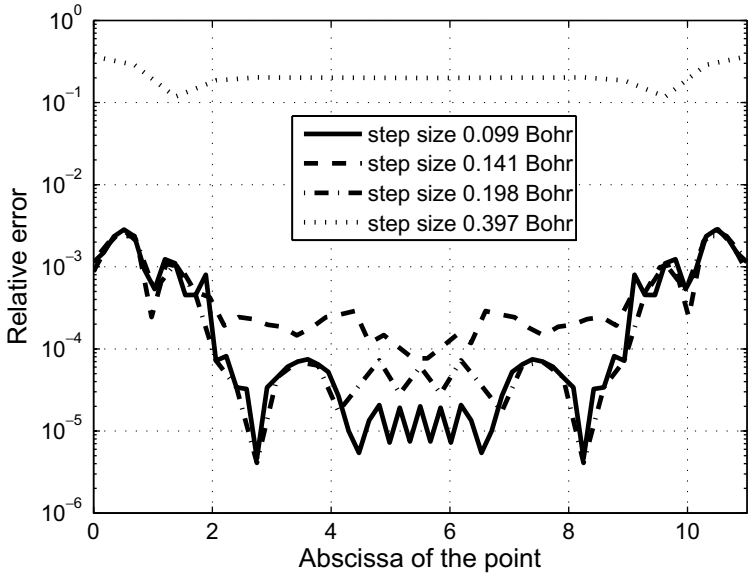


Fig. 3. difference between Abinit's result and recursion's result. The calculation refers to four Helium atoms at 150,000 K, in a cubic box of size 6.35 Bohr placed in a CFC lattice. The potential is the self-consistent potential computed by Abinit; The cut-off is 120 Hartree for the step size of 0.99 Bohr, and the number of grid points has then been divided by 2 and 4 to give the potential for step size of 0.198 Bohr and 0.397 Bohr, and the cut-off is 50 Hartree for the step size of 0141 Bohr. The chemical potential is the one computed by Abinit: $\mu = -0.59330$ Hartree. The figure draws the electronic density along the long diagonal of the cell.

structure calculations using a plane-wave method [14]. The test case have been done with a periodic cubic box of length 6.35 Bohr containing four Helium atom in a CFC lattice at 150,000 K. The atoms are at the vertex and the center of the faces, and the density have been computed along the long diagonal of the cell. The self-consistent potential and density have been computed with Abinit, using a Troullier–Martins pseudo-potential [24], the cut-off have been determined in order to achieve a maximum relative error of about $10^{-3}$ on the density.

The difference between the density computed with Abinit and the present method is drawn on Fig. 3, for different step size of the recursion. The self-consistent potential was first computed with Abinit, with a cut-off of 120 Hartree that is real space step size of 0.099 Bohr (we also used the same potential on doubled and quadrupled grids that is with grid size of 0.198 Bohr and 0.397 Bohr). Generally speaking, the convergence of the density is rather good, the maximum error being at the vertex that is, where the potential is the sharpest , and is best at the point where the potential varies slowly. We notice that the the density computed by Abinit is very sensitive to the parameters of the calculation: reducing the cut-off to 50 Hartree (grid size: 0.141 Bohr) leads to a larger variation than doubling the grid size of the recursion.

Fig. 4 compares $\frac{\prod_{i=1}^{n+1} b_i^2}{|D_n D_{n+1}|}$, the asymptotic estimate from formula (26) and the error $|\frac{N_n}{D_n} - l|$. As expected, it is not a strict upper bound of the error, but it is of the same order as the error, and this from the first recursion step: it can therefore be used in practice to stop the computation at the desired accuracy.

### 7.3. Effect of the localization

Finally, we have studied the effect of truncating $u_n$ beyond a certain radius $R_{\text{cut}}$ on the convergence in the two previous systems. For the Helium CFC, since the radius would contain all the nearest atoms of the computed point, we use a super-cell instead of only one cell. We have computed the density in a super-cell of $4 \times 4 \times 4$ cubic cell of size 25.4 Bohr, containing a total of 256 Helium atoms. In order to put these results in perspective, we also used for the free electron gas a cell of side 25.4 Bohr, and the same chemical potential.

Figs. 5 and 6 show the convergence result without truncation and for truncation radius $R_{\text{cut}}$ of 10 and 5 Bohr. As might be expected, the convergence is not changed, until we reach a point where the convergence stops, but does not deteriorate. This is probably an indication that we have achieved convergence toward the solution of the problem, with the boundary condition $u_n(|r - r_i|) = 0$ for $|r - r_i| > R_{\text{cut}}$, but this would require

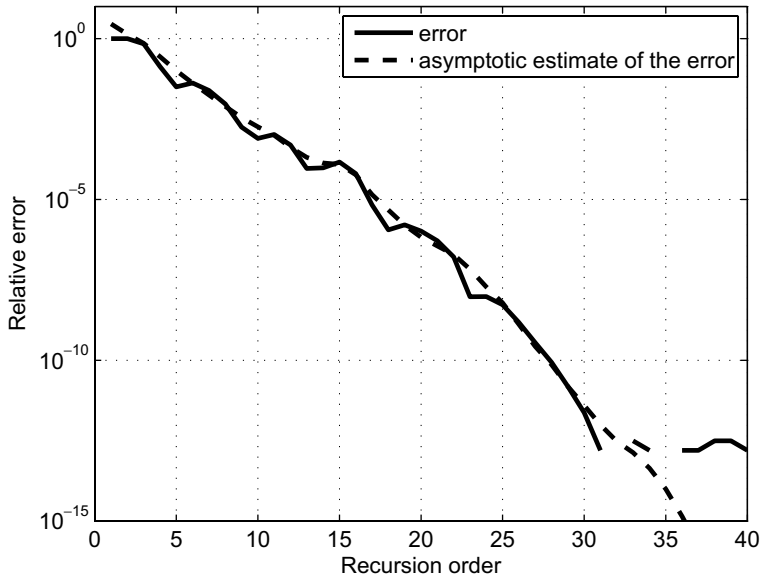


Fig. 4. Error of the recursion and equivalent of formula (26). The calculation refers to two Helium atom at 150,000 K, in a cubic box of size 6.35 Bohr placed in a CFC lattice. the potential is the self-consistent potential computed by Abinit with a cut-off of 50 Hartree, and the chemical potential computed by Abinit: $\mu = -0.59330$ Hartree. The density is calculated at a vertex of the box.

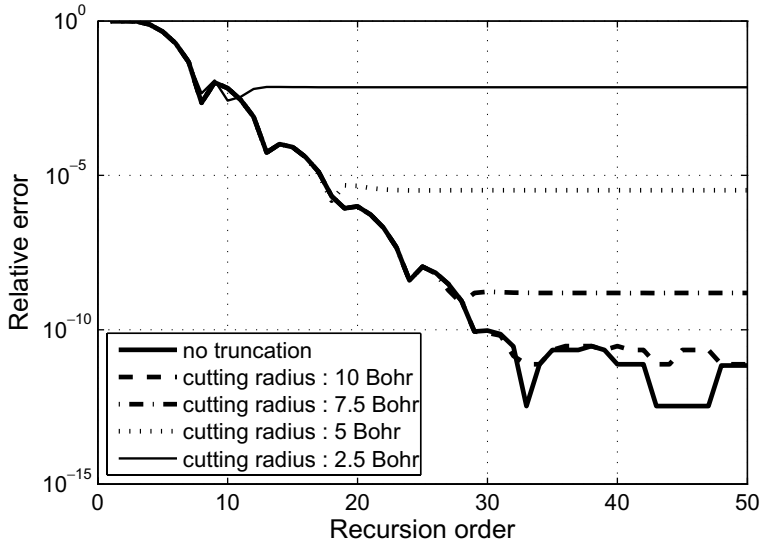


Fig. 5. Convergence of recursion method for the free electron gas for different truncation radius. The calculation refers to an electron gas at 150,000 K, a cubic box of size 25.4 Bohr and a chemical potential taken as $\mu = -0.59330$ Hartree.

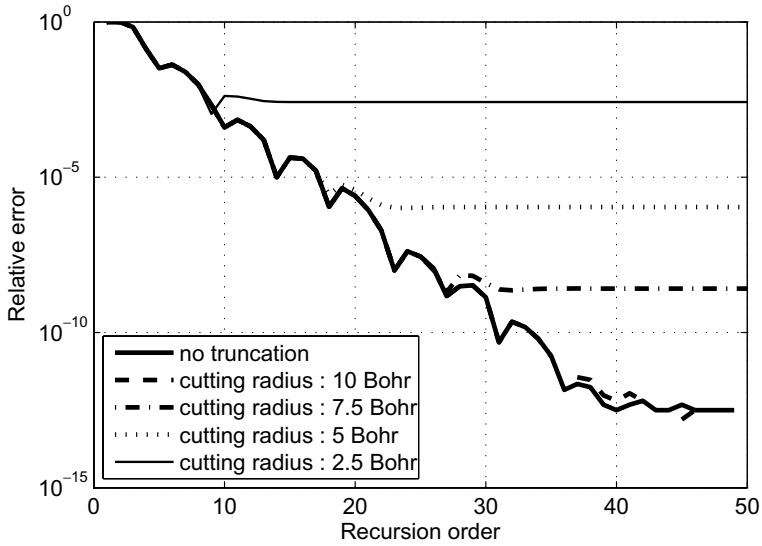


Fig. 6. Convergence of recursion method for an Helium CFC for different truncation radius. The size of the calculation box is 25.4 Bohr and contains 128 Helium atoms at 150,000 K, the chemical potential is taken as $\mu = -0.59330$ Hartree. The density is calculated at a vertex of the box.

more investigation. The final error as a function of the cut-off radius is also the same for the free electron gas and the Helium CFC: the free electron gas seems sufficient to estimate the final error as a function of the range of the recursion vector. This reflects the fact the screening length is mostly defined by the electronic density.

## 8. Conclusion

In this work, we have established some convergence properties of the recursion method first introduced in [12], and obtained what we think are interesting properties of the algorithm.

First, in spite of the various approximations incurred, it is possible to obtain quite high an accuracy, at least in the studied cases, and the convergence is smooth, linear and uniform. We think this is due to the use of the exponential of the Hamiltonian, a compact operator, for which convergence properties of the recursion coefficients is guaranteed. Second, the method is stable, truncating the $u_n$ or using a large discretization step only reduce the final precision of computation, but does not seem to affect the speed of convergence or induce instabilities. Third, an accurate and easy to compute estimate of the error has been devised, a particularly useful property when performing practical calculations.

Finally, the growth of the recursion vector, which is roughly controlled by the free electron gas term can be evaluated and, coupled with the preceding error estimate allows to effectively truncate the recursion vector and perform calculation with order N scaling.

We think this method paves the way for performing high temperature *ab initio* molecular dynamics.

**Acknowledgments**

The authors thank Ch. Lubich for exchanges on the errors bounds on Feynmann–Strang splitting, Andrew Knyatzev for discussions on eigenvalues principles, and one of the referee for his suggestion to improve our proof in Section 4. We also thank F. Alouges for discussions on continued fractions.

## Appendix A. Asymptotic error estimate

We will here prove formula (26):

$$\left|\frac{N_n}{D_n} - l\right| = \frac{\prod_{i=1}^{n+1} b_i^2}{|D_n D_{n+1}|}\left(1 + O(b_{n+2}^2)\right)$$

At this point, since we consider the expression (11) to be evaluated by continued fractions we will consider $D_n$ as a function of $z$ and use the explicit notation $D_n(z)$ only when necessary. Note that we wish to obtain estimates for $D_n(z_j)$, where $d(z_j, \mathbb{R}_+) > 0$ . If one of the $b_n$ is zeros, then the recursion stops at order $n$ and the limit is exactly reached at $n$. That formula is then verified.

Let's assume that all $b_n$ are non-zero. We first write $\frac{N_n}{D_n}$ as a series:

$$\frac{N_n}{D_n} - l = \sum_{k=n+1}^{\infty} \frac{\prod_{i=1}^{k} b_i^2}{D_k D_{k-1}} = \frac{\prod_{i=1}^{n+1} b_i^2}{D_n D_{n+1}}\left(1 + \sum_{k=n+2}^{\infty} \prod_{i=n+2}^{k} b_i^2 \frac{D_n D_{n+1}}{D_k D_{k-1}}\right)$$

It is here useful to notice that for $k \geqslant n+2$:

$$\frac{D_n D_{n+1}}{D_k D_{k-1}} = \prod_{i=n+2}^{k} \frac{D_{i-2}}{D_i}$$

And then we have:

$$\frac{N_n}{D_n} - l = \frac{\prod_{i=1}^{n+1} b_i^2}{D_n D_{n+1}}\left(1 + \sum_{k=n+2}^{\infty} \prod_{i=n+2}^{k} \left(b_i^2 \frac{D_{i-2}}{D_i}\right)\right) = \frac{\prod_{i=1}^{n+1} b_i^2}{D_n D_{n+1}}\left(1 + b_{n+2}^2 \frac{D_n}{D_{n+2}} \sum_{k=n+2}^{\infty} \prod_{i=n+3}^{k} \left(b_i^2 \frac{D_{i-2}}{D_i}\right)\right)$$

We need only to prove that $\frac{D_n}{D_{n+2}} \sum_{k=n+2}^{\infty} \prod_{i=n+3}^{k} \left(b_i^2 \frac{D_{i-2}}{D_i}\right)$ is bounded independently of $n$.

Let's assume that $|\frac{D_{i-2}}{D_i}|$ is bounded independently of $i$:

$$0 < \left|\frac{D_{i-2}}{D_i}\right| < M$$

Since $b_i$ converge to 0, we choose $n_0$ so that $|b_i^2| < \frac{1}{2M}$ for $i \geqslant n_0$. We then have for $n \geqslant n_0$:

$$\left|\frac{D_n}{D_{n+2}} \sum_{k=n+2}^{\infty} \prod_{i=n+3}^{k} \left(b_i^2 \frac{D_{i-2}}{D_i}\right)\right| < M \sum_{k=n+2}^{\infty} \prod_{i=n+3}^{k} \frac{1}{2} = 2M$$

which gives the result.

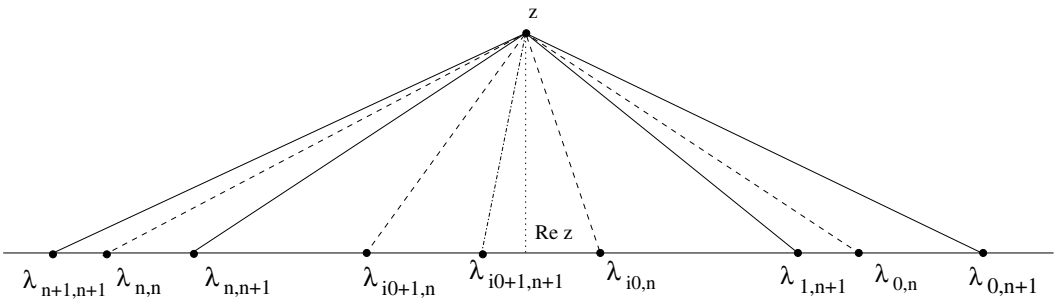


Fig. A.1. $|D_{n+1}|$ is the product of the length of the solid lines and the dot-dashed line, $|D_n|$ is the product of length of the dashed lines. Each solid line is greater than a dashed line, and the dot-dashed one is greater that $|\mathrm{Im}z|$.

We will now prove that $|\frac{D_{i-1}}{D_i}|$ is bounded, which will complete the proof.

We will use the localization of the roots of $D_n(z)$. $D_n(z)$ is the characteristic polynomial of $M_n$:

$$M_n = \begin{bmatrix} a_0 & b_1 & & \\ b_1 & a_1 & \ddots & \\ & \ddots & \ddots & b_n \\ & & b_n & a_n \end{bmatrix}$$

The localization of roots of characteristic polynomial of such matrix is known: let's write $(\lambda_{i,n})_{i=0,\ldots,n}$ the $n+1$ roots of $D_n(z)$, sorted in decreasing order:

$$\lambda_{n,n} \leqslant \lambda_{n-1,n} \leqslant \cdots \leqslant \lambda_{1,n} \leqslant \lambda_{0,n}.$$

Then the roots $(\lambda_{i,n+1})_{i=0,\ldots,n}$ of $D_{n+1}(z)$ are all distinct and strictly separated by the roots of $D_n$:

$$\lambda_{n+1,n+1} < \lambda_{n,n} < \lambda_{n,n+1} < \cdots < \lambda_{1,n+1} < \lambda_{0,n} < \lambda_{0,n+1}$$

(for proof, see [25, Chapter 5]).

The end of the proof is summarized on Fig. A.1. There is a $i_0 \in [\![ -1, n ]\!]$ so that $\lambda_{i_0+1,n} \leqslant \mathrm{Re}z < \lambda_{i_0,n}$ (with $i_0 = -1$ or $i_0 = n$ if $\mathrm{Re}z \notin [\lambda_{n,\,n}\lambda_{0,n}]$). If $j \geqslant i_0 + 1$, then $\lambda_{j+1,n+1} < \lambda_{j,n} \leqslant \mathrm{Re}z$, and then $|z - \lambda_{j,n}| < |z - \lambda_{j+1,n+1}|$. If $j \leqslant i_0$ then $\lambda_{j,n+1} > \lambda_{j,n} > \mathrm{Re}z$, and then $|z - \lambda_{j,n}| < |z - \lambda_{j,n+1}|$. It follows:

$$\begin{aligned} |D_n| = \prod_{j=0}^{n} |z - \lambda_{j,n}| &< \prod_{j=0}^{i_0} |z - \lambda_{j,n+1}| \prod_{j=i_0+1}^{n} |z - \lambda_{j+1,n+1}| < \frac{1}{|z - \lambda_{i_0+1,n+1}|} \prod_{j=0}^{n+1} |z - \lambda_{j,n+1}| < \frac{1}{|z - \lambda_{i_0+1,n+1}|} |D_{n+1}| \\ &< C|D_{n+1}| \end{aligned}$$

with $C = \frac{1}{d(z,R^+)}$. This complete the Proof.

## References

[1] S. Goedecker, Linear scaling electronic structure methods, Reviews of Modern Physics 71 (4) (1999) 1085–1123.
[2] A. Gibson, R. Haydock, J. LaFemina, Ab initio electronic-structure computations with the recursion method, Physical Review B 47 (15) (1993) 9229–9237.
[3] A. Horsfield, A. Bratkovsky, M. Fearn, D. Pettifor, M. Aoki, Bond-order potentials: theory and implementation, Physical Review B 53 (19) (1996) 12694–12712.
[4] D. Hohl, V. Natoli, D. Ceperley, R. Martin, Molecular dynamics in dense hydrogen, Physical Review Letters 71 (4) (1993) 541–544.
[5] J. Penman, J. Clérouin, P.-G. Zérah, Equation of state of a hydrogen plasma by density functional molecular dynamics, Physical Review E 51 (6) (1995) 5224–5227.
[6] L. Collins, I. Kwon, J. Kress, N. Troullier, D. Lynch, Quantum molecular dynamics simulations of hot, dense hydrogen, Physical Review E 52 (6) (1995) 6202–6219.
[7] O. Pfaffenzeller, D. Hohl, Structure and electrical conductivity in fluid high-density hydrogen, Jouranl of Physics: Condensed Matter 9 (1997) 11023–11034.
[8] F. Lambert, J. Clérouin, G. Zérah, Very-high-temperature molecular dynamics, Physical Review E 73 (1) (2006) 16403.

[9] S. Baroni, P. Giannozzi, Towards very large-scale electronic-structure calculations, Europhysics Letters 17 (1992) 547.
[10] S. Bagnier, P. Dallot, G. Zérah, Multiscale recursion in dense hydrogen plasmas, Physical Review E 61 (6) (2000) 6999–7008.
[11] R. Haydock, C. Nex, A general terminator for the recursion method, Journal of Physics C 18 (1985) 2235–2248.
[12] E. Lorin, G. Zérah, Recursion method for electronic structure calculations, Computer Physics Communications 158 (1) (2004) 39–46.
[13] B. Militzer, Shock Hugoniot Calculations of Dense Liquid Helium, American Physical Society, APS March Meeting, March 13–17, 2006, abstract# K42. 001.
[14] X. Gonze, J. Beuken, R. Caracas, F. Detraux, M. Fuchs, G. Rignanese, L. Sindic, M. Verstraete, G. Zerah, F. Jollet, et al., First-principles computation of material properties: the ABINIT software project, Computational Materials Science 25 (3) (2002) 478–492.
[15] S. Lundqvist, N. March, Theory of the Inhomogeneous Electron Gas, Plenum Press, 1983.
[16] C. Hartwigsen, S. Goedecker, J. Hutter, Relativistic separable dual-space Gaussian pseudopotentials from H to Rn, Physical Review B 58 (7) (1998) 3641–3662.
[17] B. Simon, Schrodinger semigroup, bulletin of the American Mathematical Society (NS) 7 (1982) 447–526.
[18] R. Haydock, Recursive solution of the Schroedinger equation, in: P. Ehrenreich, F. Seitz, D. Turnbull (Eds.), Solid State Physics, vol. 35, Academic, New York, 1980, p. 215.
[19] B. Dia, M. Schatzman, An estimate of the Kac transfer operator, Journal of Functional Analysis 145 (1) (1997) 108–135.
[20] T. Jahnke, C. Lubich, Error bounds for exponential operator splittings, BIT Numerical Mathematics 40 (4) (2000) 735–744.
[21] S. Descombes, M. Schatzman, Strang's formula for holomorphic semi-groups, Journal de Mathematiques Pures et Appliquees 81 (1) (2002) 93–114.
[22] C. Nex, Estimation of integrals with respect to a density of states, Journal of Physics A: Mathematical and General 11 (4) (1978) 653–663.
[23] N. Ashcroft, N. Mermin, S. Rodriguez, Solid state physics, American Journal of Physics 46 (1) (1978) 116–117.
[24] N. Troullier, J. Martins, Efficient pseudopotentials for plane-wave calculations, Physical Review B 43 (3) (1991) 1993–2006.
[25] J. Stoer, R. Bulirsch, Introduction to Numerical Analysis, Springer, 2002.